Structural, microgravimetric and voltammetric characterization of magnetron-sputtered Al–5Mg alloy

Virginija Uksienė, Konstantinas Leinartas, Remigijus Juškėnas, Aloyzas Sudavičius and Eimutis Juzeliūnas

Institute of Chemistry,
A. Goštauto 9,
LT-2600 Vilnius, Lithuania

Al–5Mg films were formed on quartz crystal substrates by magnetron sputtering technique using casting alloy as a sputtering target. The content of elements in the films was similar to that of the sputtering target. The X-ray diffraction indicated a crystalline structure of the MS deposits with a pronounced <111> texture. Initial corrosion stages of Al–5Mg in water, 3.5% NaCl solution and that containing 50 ppm Cu(II) have been studied by EQCM, which is a sensitive mass change detector with nanogram resolution. A distinctive mass gain registered by EQCM showed that alloy corrosion activity in NaCl solution was higher than in pure water. Copper cations inhibited corrosion during the first corrosion stages ($t < 1$ min), whereas with increase in immersion time the inhibition effect was changed by a strong corrosion acceleration. Copper inclusions catalyzed a partial cathodic reaction of the corrosion process, *viz*. water decomposition. Voltammetric data indicated a superior corrosion resistance of the magnetron-sputtered coatings as compared to conventional casting alloys.

Key words: aluminium-magnesium alloys, magnetron sputtering, corrosion, EQCM

INTRODUCTION

The Al–Mg alloys due to their low specific weight and high strength/weight ratio are attractive in a variety of technical applications such as food equipment, chemical processing, transport and structural fields, especially where seawater exposure is involved [1]. However, the application of these alloys is limited by susceptibility to pitting or exfoliation corrosion, which is higher than that of pure aluminium. The primary reason for the Al–Mg corrosion activity is a low protective capacity of the magnesium hydroxide film [1–3].

Magnetron-sputtering coatings attracted considerable attention in the recent years as alternatively produced environment-friendly corrosion-resistant alloys [4–27]. Sputtered alloys, due to their chemical homogeneity and amorphous or nanocrystalline structure, could be of superior anticorrosive stability than their conventional crystalline counterparts. So, increased corrosion resistance was found for sputtered Co–Cr–Mo, Ni–Cr–Mo and Fe–Cr–Ni [24–26]. However, the resistance of sputtered Au–Pd–In was similar to that of the casting alloy [22, 23]. Hashimoto et al. came to the conclusion that precipitation of nanocrystallites with dimensions less than 20 nm could increase corrosion resistance, as they have demonstrated by heat treatment of amorphous Zr–Cr and Al–Cr alloys [27, 28].

In this work, we have studied the structural, electrochemical and anticorrosive properties of magnetron-sputtered Al–5%Mg alloy in water, 3.5% NaCl solution and in the latter additionally activated by adding Cu(II). The corrosion dynamics was studied *in situ* using an electrochemical quartz crystal microbalance (EQCM), which is a commonly known sensitive mass detector capable of supplying continuous information in both gaseous and liquid environments.

EXPERIMENTAL

A commercially available Al–5Mg alloy was used as a magnetron-sputtering target. Its composition was determinated on a JXA-50A (Japan) scanning electron microscope equipped with an electron probe microanlyzer.

Quartz discs (AT plane) were used in EQCM, their fundamental frequency being f_0 = 5 MHz and d = 15 mm (produced by KVG Quartz Crystal Technology GmbH, Germany). The Al–Mg alloy was deposited on quartz substrates by a magnetron-sputtering technique.

The magnetron-sputtering chamber was vacuumed. The working gas was Ar and its pressure was maintained at 0.1–0.2 Pa. The temperature in the chamber was *ca*. 50 °C. The Ar ionisation current was 60 mA and the voltage was 450 V. The sputtering duration was 10 min, which corresponded to a coating thickness of *ca*. 0.2–0.3 μm. To prepare the thicker samples for XRD studies, the sputtering duration was extended to 15–20 min. More details about the MS procedure used are given elsewhere [22–26].

Both quartz sides were plated with the alloy; the coatings acted as excitation electrodes in the oscillation circuit. The specimens were mounted in a special window of a Teflon cell, with one of the sides exposed to the solution compartment and the other one facing air. The actual electrode area that contacted the solution was 0.78 cm^2. The EQCM experimental device was analogous to that described previously [22–26]. The EQCM measurements were started several seconds after the cell had been filled with solution. The proportion coefficient between the frequency and the mass change according to Sauerbrey's equation [29] was C = 18 ng $Hz^{-1}cm^{-2}$ at f_0 = 5 MHz.

The XPS spectra were recorded by an Escalab MK spectrometer (Great Britain), using MgK_α radiation (1253.6 eV, pass energy of 20 eV). To obtain depth profiles, the samples were etched in the preparation chamber by ionised argon at a vacuum of 5×10^{-4} Pa. An accelerating voltage of *ca*. 15 kV and a beam current of 20 μA cm^{-2} were used, which corresponded to an etching rate of *ca*. 2 nm min^{-1}.

X-ray diffraction (XRD) investigations were carried out using MoK_α radiation selected by a secondary graphite monochromator. The step-scan mode with a step 0.05° 2θ and a sampling time of 10 s/step in the range 10° ≤ 2θ ≤ 40° was used.

Triply distilled water, 3.5% NaCl and 3.5% NaCl + 50 ppm Cu(II) solutions were used as corrosion media. Analytical grade purity NaCl and $CuCl_2$ salts were used to prepare the solutions.

RESULTS AND DISCUSSION

The analysis of magnetron-sputtered coatings was performed using XPS and the results are given in Table 1. The sputtered films had a similar content of elements (*ca.* ±5%) in comparison to the bulk alloy used as a sputtering target (Table 2).

Table 1. **Composition of the Al–Mg alloy deposited on quartz crystal by magnetron sputtering. The sample were analysed by XPS**

Depth, nm	Weight %					
	Al	Mg	O	Cu	Fe	Rest
0	39.41	4.42	55.79	0.1	0.19	0.09
1	48.43	4.38	46.65	0	0.36	0.18
3	63.29	2.49	32.79	0.18	0.18	1.07
5.5	66.49	2.69	28.80	0.16	0.58	1.28
15	68.51	3.28	26.20	0	0.20	1.81
30	70.18	2.69	24.81	0	0.21	2.11

Table 2. **Composition of the Al–Mg alloy target. The sample was analysed by SEM**

Element	Weight %
Al	95.237
Mg	3.744
Si	0.376
Pb	0.007
Bi	0.001
Zn	0.046
Cu	0.031
Ni	0.004
Co	0.001
Fe	0.329
Mn	0.169
Cr	0.041
V	0.001
Ti	0.011
Sn	0.001

The X-ray diffraction (XRD) patterns of the sputtered coating and the casting alloy are shown in Fig. 1. Sharp XRD peaks indicate a perfect crystalline structure of both alloys (the peaks are indexed). The specimens have the same cubic face-centred lattice type typical of Al, but a different texture: the sputtered deposit has the pronounced texture in <111> direction, while the cast is characterized by the texture <110> and <311>.

Figure 2 shows the mass change dynamics registered by EQCM after Al–Mg immersion in different corrosion media: pure water, 3.5% NaCl solution and 3.5% NaCl + 50 ppm Cu(II). The general EQCM response is mass gain, what implies accumulation of corrosion products on the corroding surface. The mass gain in NaCl solution is greater than in pure water, indicating a higher corrosion activity in the presence of chloride ions. A high

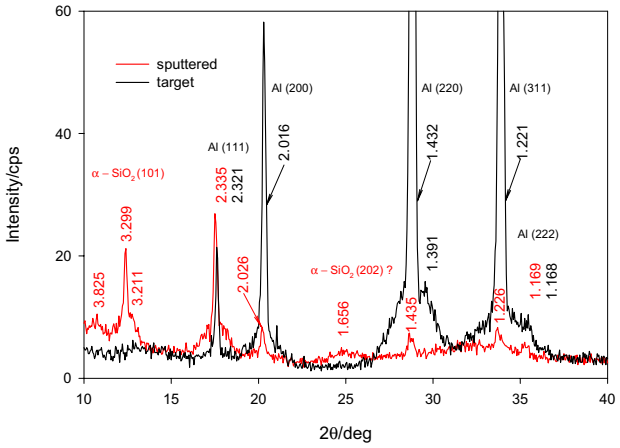

Fig. 1. XRD patterns for casting Al–Mg alloy (a) and magnetron sputtered one (2 μm in thick) on quartz crystal specimen. MoK_α radiation

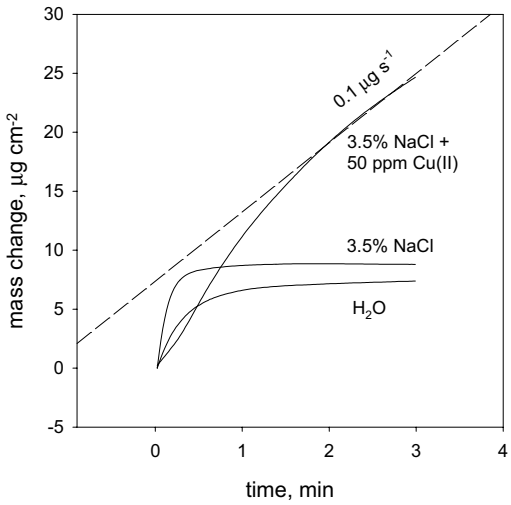

Fig. 2. Al–Mg mass change determined by EQCM during corrosion in pure water, 3.5% NaCl and 3.5% NaCl + + 50 ppm Cu(II)

corrosion rate is observed in both media during the first corrosion stages. With the time, corrosion activity decays, and after *ca*. 2 min the rate of mass change becomes very low, indicating a very high corrosion stability of the sputtered alloy.

A serious technical is problem is Al–Mg alloy exploitation in media containing low concentrations of heavy metal cations, *e.g.* Cu(II), which can accelerate corrosion. The initial corrosion rate in NaCl+Cu(II) solution is lower than in pure water or copper-free NaCl solution (Fig. 2). However, after a certain time ($t > 1$ min), a strong Cu(II) accelerating effect becomes evident. Such an change of inhibition by acceleration agrees with the results obtained in [31]. The authors investigated the role of various heavy metal cations on aluminum corrosion and came to the conclusion that the cations caused inhibition at low concentrations (in our experiment at a shorter immersion time), while at higher concentrations (at a longer time) a strong acceleration effect took place.

Aluminium corrosion consists of the anodic oxidizing reaction

$$2Al + H_2O \rightarrow Al_2O_3 + 6H^+ + 6e \quad (E° = -1.55\ V) \quad (1)$$

and cathodic water decomposition

$$2H_2O + 2e \rightarrow H_2 + 2OH^- \quad (E° = -0.828\ V) \quad (2)$$

By definition, cathodic oxygen reduction is also possible

$$O_2 + 2H_2O + 4e \rightarrow 4OH^- \quad (E° = -0.401\ V) \quad (3)$$

Magnesium corrosion may be described by anodic dissolution

$$Mg \rightarrow Mg^{2+} + 2e \quad (E° = -2.37\ V) \quad (4)$$

and cathodic water decomposition (2). These electrochemical reactions in neutral solutions could be accompanied by hydroxide precipitation:

$$Mg^{2+} + 2(OH)^- \rightarrow Mg(OH)_2. \quad (5)$$

(Let us remember that the solubility of $Mg(OH)_2$ in water at 18 °C is 0.09 g l^{-1} [32].)

In Cu(II) solutions, deposition of copper takes place on Al–Mg surface:

$$Cu^{2+} + 2e \rightarrow Cu \quad (E° = 0.342\ V). \quad (6)$$

The copper deposits on the Al–Mg surface exposed to 50 ppm Cu(II) solution are shown on SEM micrographs (Fig. 3). The formations have a cauliflower shape with dimensions of some micrometers. A nobler copper on the less noble Al–Mg represents a system of micro-cathodes, on which water decomposition (2) is accelerated. As a result, the coupled anodic reactions (1) and (4) are accelerated as well. The SEM micrograph shows inherent domains of localised corrosion (corrosion pits), which developed during the copper-enhanced corrosion.

Both the oxide (1) and the hydroxide (5) formation as well as copper deposition (6) may contribute to the mass gain registered by EQCM in Cu(II) solution (Fig. 2). In order to discriminate between those contributions, XPS surface analysis was un-

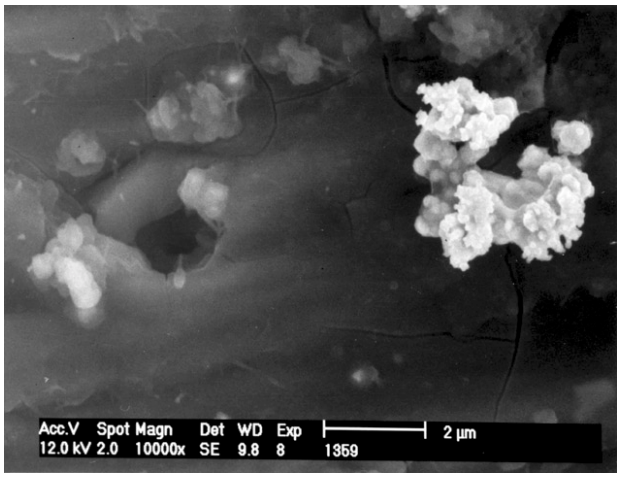

Fig. 3. SEM micrographs of the copper deposit and corrosion pit on the Al–Mg surface exposed for 20 min to 3.5% NaCl + 50 ppm Cu(II) solution

dertaken, using surface etching by ionised argon. Figure 4 shows the depth profile data of the surface layer developed on Al–Mg in 50 ppm Cu(II) solution (the metal contents include both oxidized (Me^{z+}) and metallic (Me) forms). Obviously, aluminium oxide predominates in the surface layer. The aluminium-oxygen content in the outermost layer (d = = 0 nm) makes about 93% in mass ([Al] = 29.8% and [O] = 63.58%). Aluminium content increases and oxygen content decreases in deeper levels.

The outermost layer (d = 0–10 nm) contains about 2–4% of copper. Approaching deeper levels, the copper content increases to *ca.* 10% (d = 30–120 nm) and then decreases again to a few mass percent.

A symptomatic feature is that the surface layer contains a very small amount of magnesium. While the magnesium concentration in the alloy is about 5%, its content in the corrosion product layer is below 1% at d = 0–120 nm (Fig. 4). This means that a significant part of magnesium is transferred to solution phase during corrosion.

Thus, it can be concluded that the mass gain measured by EQCM during corrosion in the Cu(II) solution (Fig. 2) is mainly due to formation of aluminium oxide layer. According to XPS analysis, the contribution of copper to total mass gain is below 10% and the contribution of magnesium is insignificant.

The voltammetric curves were obtained for both magnetron-sputtered and casting alloys in a 3.5% NaCl solution as well as in that containing 50 ppm Cu(II) (Figs. 4 and 5). These data clearly indicate a higher resistance of the sputtered alloy in both

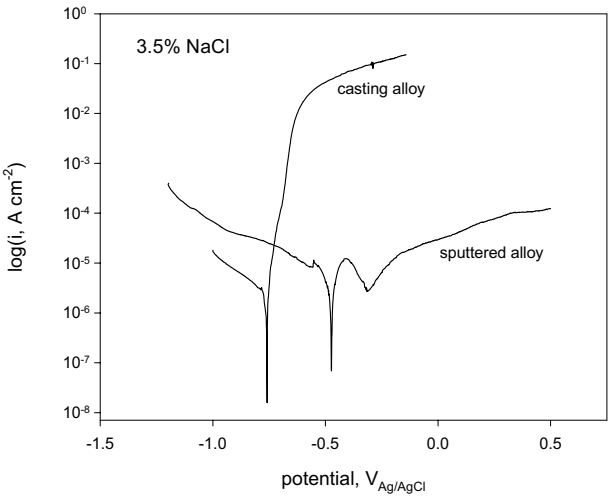

Fig. 5. Potentiodynamic curves (v = 5 mV s^{-1}) obtained for casting Al–5Mg alloy and magnetron sputtered one in 3.5% NaCl. Immersion time 10 min.

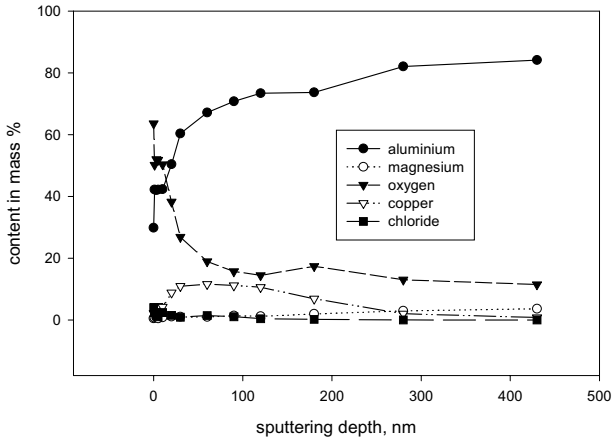

Fig. 4. Content of the elements determined by XPS and surface sputtering by ionised argon of the surface layer on Al–Mg exposed for 20 min to 3.5% NaCl + 50 ppm Cu(II).

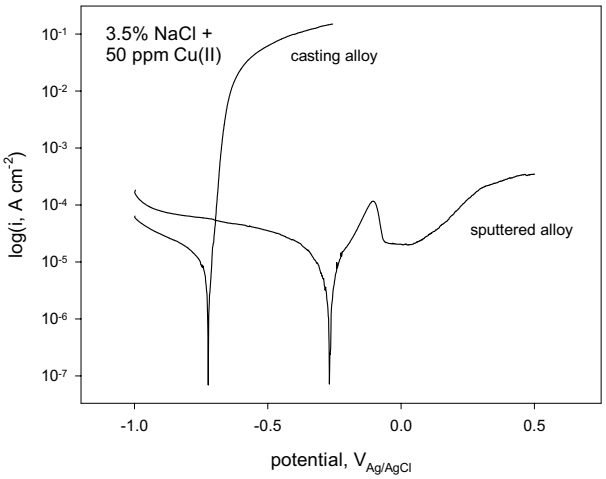

Fig. 6. Potentiodynamic curves (v = 5 mV s^{-1}) obtained for casting Al–5Mg alloy and magnetron sputtered one in 3.5% NaCl + 50 ppm Cu(II). Immersion time 10 min.

solutions. The sputtered alloy is characterized by a much higher value of the open circuit potential and a much lower anodic activity as compared to those of the casting alloy. In our previous investigations, it has been shown by electrochemical impedance spectroscopy (EIS) that sputtered deposits usually have 2–3 times larger actual surface areas than the mechanically treated alloys [23, 24, 26]. To the same conclusion lead the voltammetric data in Figs. 4 and 5. The cathodic currents have to be attributed mainly to hydrogen evolution (2). These currents are several times higher on the sputtered specimens, in accordance with the proposition about a larger actual area of the sputtered surfaces.

CONCLUSIONS

An XPS depth profile analysis showed that the chemical composition of the magnetron-sputtered Al–Mg deposits was similar to that of the casting alloy used as an MS target. X-ray diffraction investigations indicated a crystalline structure of the MS deposits with a pronounced <111> texture.

A microgravimetric Al–Mg corrosion sensor was prepared by dc magnetron sputtering of the alloy on quartz crystal specimens. EQCM measurements indicated that the Al–Mg corrosion activity in 3.5% NaCl was higher than in pure water. Copper cations ($c_{Cu(II)}$ = 50 ppm) caused corrosion inhibition during the first corrosion stages, while after some time a strong corrosion acceleration was observed.

SEM investigations showed the presence of the cauliflower-like copper deposits with the size of a few micrometers on Al–Mg surface exposed to Cu(II) solution. The XPS analysis data indicated that the layer on the corroded surface was composed mainly of aluminum oxide, whereas the copper content was below 10% and that of magnesium negligible. The copper deposits acted during corrosion as a system of micro-cathodes, on which water decomposition was accelerated.

ACKNOWLEDGEMENTS

The skilful assistance of P. Gawenda (Karl-Winnacker-Institut der DECHEMA e.V., Germany) in SEM experiments is highly appreciated. V. Lisauskas is greatly acknowledged for the contribution in preparation of the microgravimetric samples.

Received 13 May 2002
Accepted 20 Juny 2002

References

1. D. A. Jones, Principles and Prevention of Corrosion. Prentice-Hall, Inc. Upper Saddle River, NJ 07458. 1996.
2. E. Brillas, P. L. Cabot, F. Centellas, J. A. Garrido, E. Perez, and R. M. Rodriguez, *Electrochim. Acta* **43**, 799 (1998).
3. J. H. Nordlien, K. Nisancioglu, S. Ono, and N. Masuko, *J. Electrochem. Soc.* **143**, 2564 (1996).
4. X.-Y. Li, E. Akiyama, H. Habazaki, A. Kawashima, K. Asami, and K. Hashimoto, *Corros. Sci.* **41**, 1849 (1999).
5. G. S. Frankel, R. C. Newman, C. V. Jahnes, M. and A. Russak. *J. Electrochem. Soc.* **140**, 2192 (1993).
6. H. Habazaki, K. Shimizu, P. Skeldon, G. E. Thompson, and G. C. Wood. *Thin Solid Films* **300**, 131 (1997).
7. H. Habazaki, K. Takahiro, S. Yamaguchi, K. Shimizu, P. Skeldon, G. E. Thompson, and G. C. Wood, *J. Electrochem. Soc.* **146**, 2502 (1999).
8. H. Habazaki, P. Skeldon, G. E. Thompson, G. C. Wood, and K. Shimizu, *J. Mater. Res.* **12**, 1885 (1997).
9. H. Habazaki, K. Shimizu, P. Skeldon, G. E. Thompson, and G. C. Wood, *Corros. Sci.* **39**, 731 (1997).
10. H. Habazaki, P. Skeldon, G. E. Thompson, J. Wan, G. C. Wood, X. Zhou, J. Delaet, and K. Shimizu, *J. Electrochem. Soc.* **144**, 4217 (1997).
11. M. P. Ryan, N. J. Laycock, H. S. Isaacs, and R. C. Newman, *J. Electrochem. Soc.* **146**, 91 (1999).
12. Z. Y. Liu, W. Gao, K. L. Dahm, and F. H. Wang, *Acta Materialia* **46**, 1691 (1998).
13. D. Landolt, C. Robyr, and P. Mettraux, *Corrosion* **54**, 772 (1998).
14. P. Schmutz and D. Landolt, *Corros. Sci.* **41**, 2143 (1999).
15. J. C. Oliveira, A. Cavaleiro, and C. M. A.Brett, *Corros. Sci.* **42**, 1881 (2000).
16. M. Yamasaki, H. Habazaki, K. Asami, and K. Hashimoto, *J. Electrochem. Soc.* **147**, 4502 (2000).
17. H. Mitsui, H. Habazaki, K. Asami, K. Hashimoto, and S. Mrowec, *Corros. Sci.* **38**, 1431 (1996).
18. M. Mehmood, E. Akiyama, H. Habazaki, A. Kawashima, K. Asami, and K. Hashimoto, *Corros. Sci.* **41**, 1871 (1999).
19. J. Bhattarai, E. Akiyama, H. Habazaki, A. Kawashima, K. Asami, and K. Hashimoto, *Corros. Sci.* **40**, 19 (1998).
20. J. Bhattarai, E. Akiyama, H. Habazaki, A. Kawashima, K. Asami, and K. Hashimoto, *Corros. Sci.* **40**, 155 (1998).
21. E. Juzeliūnas, K. Leinartas, M. Samulevičienė, D. Jelinskienė, A. Sudavičius, P. Miečinskas, V. Lisauskas, and B. Vengalis. In: ICCE/7 (Seventh Abnnual International Conference on Composites Engineering), Denver, Colorado, USA, 405 (2000).
22. K. Leinartas, M. Samulevičienė, A. Bagdonas, A. Sudavičius, V. Lisauskas, and E. Juzeliūnas. *Electrochem. Communications* **3**, 494 (2001).
23. K. Leinartas, P. Miečinskas, A. Sudavičius, D. Jelinskienė, R. Juškėnas, V. Lisauskas, B. Vengalis, and E. Juzeliūnas. *J. Appl. Electrochem.* **31**(10), 1079 (2001).

24. E. Juzeliūnas, K. Leinartas, M. Samulevičienė, A. Sudavičius, P. Miečinskas, R. Juškėnas, and V. Lisauskas. *J. Solid State Electrochem* (On-line publication DOI 10.1007/s100080100237).
25. E. Juzeliūnas, K. Leinartas, M. Samulevičienė, P. Miečinskas, R. Juškėnas, and A. Sudavičius. *Corros. Sci.* **44**, 1541 (2002).
26. K. Leinartas, M. Samulevičienė, A. Bagdonas, A. Sudavičius, V. Lisauskas, and E. Juzeliūnas. *Chemija* (in press).
27. V. Uksienė, K. Leinartas, A. Sudavičius, R. Juškėnas, K. Jüttner, W. Fürbeth, and E. Juzeliūnas, *Corros. Sci.* (submitted).
28. M. Mehmood, E. Akiyama, H. Habazaki, A. Kawashima, K. Asami, and K. Hashimoto, *Corros. Sci.* **40**, 1 (1998).
29. M. Mehmood, E. Akiyama, H. Habazaki, A. Kawashima, K. Asami, and K. Hashimoto, *Corros. Sci.* **41**, 477 (1999).
30. G. Sauerbrey, *Z. Phys.* **155**, 206 (1959).
31. M. G. A. Khedr and A. M. S. Lashien, *Corros. Sci.* **33**, 137 (1992).
32. Handbook of Chemistry and Physics, Ed. D. R. Lide, 73rd Edition, 1992–1993.

V. Uksienė, K. Leinartas, R. Juškėnas, A. Sudavičius, E. Juzeliūnas

STRUKTŪRINIS, MIKROGRAVIMETRINIS IR VOLTAMPERINIS MAGNETRONINIO DULKINIMO METODU SUFORMUOTŲ Al–5Mg DANGŲ APIBŪDINIMAS

S a n t r a u k a

Ant kvarco kristalo magnetroninio dulkinimo būdu suformuotos Al–5Mg dangos. Rentgeno fotoelektroninės spektroskopijos metodu ištirta, kad dangos ir taikinio – metalurginio lydinio – elementinės sudėtys yra tapačios. Rentgeno difrakcijos metodu nustatyta, kad magnetroninio dulkinimo metodu gautos Al–5Mg dangos pasižymi <111> tekstūra. Pradinės Al–5Mg lydinio korozijos stadijos buvo tirtos tris kartus distiliuotame vandenyje, 3,5% NaCl ir 3,5% NaCl + 50 ppm Cu(II) tirpaluose EKKM metodu, kuris yra jautrus nanograminiams masės pokyčiams. Elektrodų masės augimas parodė, kad lydinys yra koroziškai aktyvesnis NaCl tirpale nei gryname vandenyje. Vario katijonai stabdo koroziją pradiniu momentu (t < 1 min), o esant ilgesniam imersijos laikui korozijos greitis didėja. Vario priemaišos dalinai katalizuoja korozinio proceso katodinę reakciją, t. y. vandens skaldymą. Voltamperiniai matavimai parodė geresnį magnetroninio dulkinimo būdu gautų dangų korozinį atsparumą, palyginus su metalurginiu lydiniu.